Tau-sneutrino next-to-lightest supersymmetric particle and multilepton signatures at the LHC

Terrance Figy,[1] Krzysztof Rolbiecki,[2] and Yudi Santoso[3]
[1]*TH Division, CERN, Geneva, Switzerland*
[2]*Institute for Particle Physics Phenomenology, Durham University, Durham DH1 3LE, UK*
[3]*Department of Physics and Astronomy, University of Kansas, Lawrence, Kansas 66045-7582, USA*
(Received 3 June 2010; published 27 October 2010)

In models with gravitino as the lightest supersymmetric particle (LSP), the next-to-lightest supersymmetric particle (NLSP) can have a long lifetime and appear stable in collider experiments. We study the leptonic signatures of such a scenario with tau sneutrino as the NLSP, which is realized in the non-universal Higgs masses (NUHM) scenario. We focus on an interesting trilepton signature with two like-sign taus and an electron or a muon of the opposite sign. The neutralinos and charginos are quite heavy in the model considered, and the trilepton signal comes mostly from the slepton-sneutrino production. We identify the relevant backgrounds, taking into account tau decays, and devise a set of cuts to optimize this trilepton signal. We simulate signal and backgrounds at the Large Hadron Collider (LHC) with 14 TeV center-of-mass energy. Although the sleptons in this model are relatively light, $\mathcal{O}(100\ \mathrm{GeV})$, discovery is more demanding compared to typical neutralino LSP scenarios. The trilepton signal requires a large amount of accumulated data, at least $\sim 80\ \mathrm{fb}^{-1}$, at the center-of-mass (c.m.) energy of 14 TeV.

DOI: 10.1103/PhysRevD.82.075016 PACS numbers: 12.60.Jv, 14.80.Ly

I. INTRODUCTION

Supersymmetry (SUSY) is one of the candidates for beyond the standard model (SM) theory that is extensively searched for at collider experiments (see, e.g., [1]). If supersymmetry does exist at the weak scale, some supersymmetric particles are expected to be produced by the Large Hadron Collider (LHC) experiment. To discover any supersymmetric signal, we need a correct theoretical interpretation of the data, and there have been many studies on this subject. However, most of these studies assume that the lightest neutralino is the stable lightest supersymmetric particle (LSP),[1] motivated by its feasibility as a dark matter particle [2]. Nonetheless, the neutralino is not the only candidate for dark matter within supersymmetry. It has been shown that a gravitino LSP can also be a good candidate for dark matter [3,4]. In this case, due to its very weak interactions, the gravitino itself would not be seen directly, while the next-to-lightest supersymmetric particle (NLSP) would appear as a stable particle at colliders.[2]

The gravitino dark matter scenario opens up many new phenomenologies with various possible NLSPs. If a sneutrino is the NLSP, all other sparticles that are produced at colliders would quickly cascade decay to the sneutrino, giving rise to jets and/or leptons along the way, while the sneutrino itself would yield a large missing energy signature in the detectors. Although this is similar to a neutralino LSP scenario, the mass spectrum, production rates, and branching ratios are in general different, leading to different characteristics. Therefore, a dedicated study for the sneutrino NLSP scenario at colliders is justified. Specifically, we look at a sneutrino NLSP scenario within a supergravity model with non-universal Higgs masses (NUHM). A preliminary study on a similar model but within gauge mediated symmetry-breaking framework has been performed by Covi and Kraml in [5], and recently also analyzed by Katz and Tweedie in [6]. In this paper, we look into a detailed analysis, involving Monte Carlo simulation, of a particular model with tau sneutrino as the NLSP. We focus on leptonic channels in order to find distinguishing signatures of the model, and we study whether the signals in such scenarios can be observed at the LHC.

For hadron colliders, supersymmetric signals can be classified as jets plus missing energy ($\not{E}_T$) [7], jets plus leptons plus missing energy, or leptons plus missing energy without a jet [8]. Because of the nature of hadron colliders, signals involving jets are expected to have higher event rates. However, the SM backgrounds for these types of events are also generally larger. On the other hand, although with relatively small event rates, isolated multilepton plus missing energy signatures offer relatively clean signals, which in some cases can be observed above the SM background. For example, a trilepton signature has been proposed as a promising channel to discover supersymmetry with a neutralino as the LSP. Motivated by this, and also because the lightest effectively stable particle in our model is leptonic, we look at signals with leptons. We found that the trilepton signature in our model provides an interesting channel, which can be used to distinguish it from many other models. However, search for this signal at the LHC, and hadron colliders in general, is hindered by the tau identification problem. On the other hand, inclusive

[1]The LSP is stable if R-parity is conserved, which we also assume in this paper.
[2]Because of its long lifetime, the NLSP would decay outside of the detectors and appear to be stable.

analysis, including jets, shows that the LHC at 14 GeV should be capable of discovering the new physics beyond the SM.

The outline of this paper is as follows. In Sec. II, we specify our model and its features, including the sparticle mass spectrum, decay branching ratios, and production rates. In Sec. III, we explore the multilepton signatures of our model. Section IV consists of discussions on the trilepton signals and backgrounds. In Sec. V, we show the results of our simulation analysis for the LHC. We conclude with Sec. VI.

II. THE MODEL AND ITS FEATURES

For our analysis, we take a specific set of parameters in the NUHM model [9]. The free parameters in this model are the universal gaugino $m_{1/2}$ and sfermion masses m_0, and the trilinear coupling A_0 (all three at the grand unified theory scale); the ratio of the two Higgs vevs $\tan\beta$; the Higgs mixing parameter μ; and the CP-odd Higgs mass m_A (at the weak scale). It has been shown that sneutrino NLSP is natural in NUHM in the sense that it has large parameter space regions allowed by all known constraints from cosmology, dark matter, and particle physics [10]. Our choice of a model corresponds to NUHM parameters $\tan\beta = 10$, $m_0 = 100$ GeV, $m_{1/2} = 500$ GeV, $A_0 = 0$, $\mu = 600$ GeV, and $m_A = 2000$ GeV. It has tau sneutrino $\tilde{\nu}_\tau$ as the NLSP and relatively light slepton masses, while the squarks and gluino are around 1 TeV, still within the reach of the LHC. The full mass spectrum is listed in Table I. Note that we use a slightly different value of m_t from the one used in [10].

We assume that the gravitino mass is lower than $m_{\tilde{\nu}_\tau}$, but we do not need to specify its value, as it is not relevant here. The lifetime of $\tilde{\nu}_\tau$ depends on the mass gap between gravitino $\tilde{G}$ and the tau sneutrino. However, since the dominant decay channel of tau sneutrino is $\tilde{\nu}_\tau \to \tilde{G} + \nu$, the tau sneutrino would still appear as missing energy even if it decays inside the detector.

Among the lighter sparticles, we have the following mass hierarchy:

$$m_{\tilde{\chi}_2^0}, m_{\tilde{\chi}_1^\pm} > m_{\tilde{\chi}_1^0} > m_{\tilde{\ell}_L} > m_{\tilde{\nu}_\ell} > m_{\tilde{\tau}_1} > m_{\tilde{\nu}_\tau}, \quad (1)$$

with $\tilde{\nu}_\tau$ as the lightest one. Note that the first two generations are mass degenerate in the model considered. Throughout this paper, we define $\ell \equiv e, \mu$, while $\ell' \equiv e, \mu, \tau$. The decay modes for these lighter sparticles are as follows. The chargino can decay as

$$\tilde{\chi}_1^\pm \to \tilde{\chi}_1^0 + W^\pm, \quad \tilde{\ell}_L + \nu_\ell, \quad \tilde{\nu}_\ell + \ell, \quad \tilde{\tau}_1 + \nu_\tau, \quad \tilde{\nu}_\tau + \tau. \quad (2)$$

For the neutralinos, the decay modes are

$$\tilde{\chi}_{1,2}^0 \to \tilde{\ell}_L + \ell, \quad \tilde{\nu}_\ell + \nu_\ell, \quad \tilde{\tau}_1 + \tau, \quad \tilde{\nu}_\tau + \nu_\tau, \quad (3)$$

while for the second-lightest neutralino, we have the additional decay mode

TABLE I. The sparticle and Higgs masses of the model we analyze. We assume top pole mass $m_t = 172.4$ GeV [11] and $m_b(m_b)^{\overline{\rm MS}} = 4.25$ GeV. The Higgs masses are calculated using FEYNHIGGS [12].

	Mass [GeV]
$m_{\tilde{\nu}_e}$	140.6
$m_{\tilde{\nu}_\tau}$	90.5
$m_{\tilde{e}_L}$	161.4
$m_{\tilde{\tau}_1}$	115.3
$m_{\tilde{\chi}_1^0}$	206.5
$m_{\tilde{\chi}_1^\pm}$	396.0
$m_{\tilde{\chi}_2^0}$	396.1
	Mass [GeV]
$m_{\tilde{\chi}_3^0}$	−617.4
$m_{\tilde{\chi}_4^0}$	633.0
$m_{\tilde{\chi}_2^\pm}$	633.5
$m_{\tilde{e}_R}$	482.7
$m_{\tilde{\tau}_2}$	459.6
$m_{\tilde{t}_1}$	723.6
$m_{\tilde{t}_2}$	994.7
$m_{\tilde{b}_1}$	956.4
$m_{\tilde{b}_2}$	1000.9
$m_{\tilde{u}_R}$	925.6
$m_{\tilde{u}_L}$	1033.4
$m_{\tilde{d}_R}$	1012.7
$m_{\tilde{d}_L}$	1036.5
$m_{\tilde{g}}$	1176.2
	Mass [GeV]
m_h	115.9
m_H	2000
m_A	2000
$m_H^\pm$	2002

$$\tilde{\chi}_2^0 \to \tilde{\chi}_1^0 + (Z, h), \quad (4)$$

although with small branching ratios.[3] It is worth noting that the decay modes for $\tilde{\chi}_1^\pm$ and $\tilde{\chi}_2^0$ are similar to that in scenarios with $\tilde{\chi}_1^0$ as the LSP. On the other hand, $\tilde{\ell}_L$ exhibits a completely different decay pattern,

$$\begin{aligned} &\tilde{\ell}_L \to \tilde{\nu}_\ell + \bar{f}' + f, \qquad \tilde{\tau}_1 + \ell + \tau, \\ &\tilde{\tau}_1 + \nu_\ell + \nu_\tau, \qquad \tilde{\nu}_\tau + \ell + \nu_\tau, \qquad \tilde{\nu}_\tau + \nu_\ell + \tau. \end{aligned} \quad (5)$$

Note that only 3-body decay channels are open for the selectron/smuon. This is because the mass gap between $\tilde{\ell}_L$ and $\tilde{\nu}_\ell$ is smaller than m_W, and also because of the flavor difference between the selectron and the NLSP. The decays

[3]Note that $\tilde{\chi}_2^0$ can also decay through a loop to $\tilde{\chi}_1^0 + \gamma$ [13]. However, this is subdominant as compared to the tree-level two-body decay modes above.

TABLE II. Decays and the total widths of $\tilde{\chi}_1^+$, $\tilde{\chi}_{1,2}^0$, $\tilde{e}_L^-$, $\tilde{\nu}_\ell$, and $\tilde{\tau}_1$. Only decays with BR $\gtrsim 1\%$ are included. The decay pattern for smuon $\tilde{\mu}_L^-$ is analogous to that for selectron $\tilde{e}_L^-$. Here, q_u, q_d represent u-, c- and d-, s-quarks, respectively. Each antiparticle has the same decay pattern as its corresponding particle.

$\tilde{\chi}_1^+ \to$	$\tilde{\nu}_\tau \tau^+$	$\tilde{\nu}_\ell \ell^+$	$\tilde{\tau}_1^* \nu_\tau$	$\tilde{\ell}_L^* \nu_\ell$	Γ [GeV]
BR [%]	18.7	2×15.9	18.5	2×15.3	7.0

$\tilde{\chi}_{1,2}^0 \to$	$\tilde{\nu}_\tau \bar{\nu}_\tau$ + c.c.	$\tilde{\nu}_\ell \bar{\nu}_\ell$ + c.c.	$\tilde{\tau}_1^* \tau^-$ + c.c.	$\tilde{\ell}_L^* \ell^-$ + c.c.	Γ [GeV]
BR ($\tilde{\chi}_1^0$) [%]	2×17.1	4×7.5	2×10.9	4×3.5	0.5
BR ($\tilde{\chi}_2^0$) [%]	2×9.1	4×7.8	2×9.5	4×7.8	7.0

$\tilde{e}_L^- \to$	$\tilde{\nu}_\tau^* \tau^- \nu_e$	$\tilde{\nu}_e q_d \bar{q}_u$	$\tilde{\nu}_e \bar{\nu}_e e^-$	$\tilde{\nu}_e \bar{\nu}_\mu \mu^-$	$\tilde{\nu}_e \bar{\nu}_\tau \tau^-$	$\tilde{\tau}_1 \tau^+ e^-$	$\tilde{\tau}_1^* \tau^- e^-$	Γ [keV]
BR [%]	30.0	2×22.0	7.7	7.3	7.3	1.0	1.0	12

$\tilde{\nu}_\ell \to$	$\tilde{\nu}_\tau \bar{\nu}_\tau \nu_\ell$, $\tilde{\nu}_\tau^* \nu_\tau \nu_\ell$	$\tilde{\nu}_\tau \tau^+ \ell^-$	$\tilde{\tau}_1^* \nu_\tau \ell^-$	Γ [keV]
BR [%]	70.1	21.0	8.4	0.4

$\tilde{\tau}_1^- \to$	$\tilde{\nu}_\tau \bar{\nu}_\ell \ell^-$	$\tilde{\nu}_\tau \bar{\nu}_\tau \tau^-$	$\tilde{\nu}_\tau q_d \bar{q}_u$	Γ [keV]
BR [%]	2×11.1	11.0	2×33.3	17.2

TABLE III. Cross sections in fb for (a) slepton pair, (b) chargino and neutralino pair, and (c) squarks and gluino production at the Tevatron and LHC with c.m. energies 7, 10, and 14 TeV. The calculation was done with HERWIG++ [17]. Note that squarks and gluino are too heavy to be produced at the Tevatron. Here, $\tilde{q}$ represents the sum over the light squarks $\tilde{u} + \tilde{d} + \tilde{s} + \tilde{c}$, while $\tilde{\ell}$ can be either $\tilde{e}$ or $\tilde{\mu}$.

(a)	$\tilde{\ell}_L^+ \tilde{\ell}_L^-$	$\tilde{\nu}_\ell \tilde{\nu}_\ell^*$	$\tilde{\ell}_L^+ \tilde{\nu}_\ell$	$\tilde{\ell}_L^- \tilde{\nu}_\ell^*$	$\tilde{\tau}_1^+ \tilde{\tau}_1^-$	$\tilde{\tau}_1^+ \tilde{\nu}_\tau$	$\tilde{\tau}_1^- \tilde{\nu}_\tau^*$	$\tilde{\nu}_\tau \tilde{\nu}_\tau^*$
Tevatron	2.9	4.7	4.4	4.4	13	28	28	34
7 TeV LHC	15	26	48	22	57	205	109	153
10 TeV LHC	29	48	86	45	100	344	201	261
14 TeV LHC	51	83	144	81	165	545	339	421

(b)	$\tilde{\chi}_1^0 \tilde{\chi}_1^0$	$\tilde{\chi}_1^0 \tilde{\chi}_1^-$	$\tilde{\chi}_1^0 \tilde{\chi}_1^+$	$\tilde{\chi}_2^0 \tilde{\chi}_1^-$	$\tilde{\chi}_2^0 \tilde{\chi}_1^+$	$\tilde{\chi}_2^0 \tilde{\chi}_2^0$	$\tilde{\chi}_1^- \tilde{\chi}_1^+$
Tevatron	0.03	0.002	0.002	0.07	0.07	0.002	0.17
7 TeV LHC	0.3	0.03	0.11	2.9	8.2	0.19	5.5
10 TeV LHC	0.7	0.08	0.26	7.8	19	0.6	14.2
14 TeV LHC	1.3	0.18	0.5	17	38	1.4	30

(c)	$\tilde{q} \tilde{q}^*$	$\tilde{q} \tilde{q}$	$\tilde{t}_1 \tilde{t}_1^*$	$\tilde{g} \tilde{q}$	$\tilde{g} \tilde{g}$	$\tilde{\chi}_1^0 \tilde{q}$	$\tilde{\chi}_2^0 \tilde{q}$	$\tilde{\chi}_1^+ \tilde{q}$	$\tilde{\chi}_1^- \tilde{q}$
7 TeV LHC	4.4	27	1.4	6.6	0.2	1.0	0.7	1.0	0.3
10 TeV LHC	34	126	9.4	79	4.1	3.9	3.4	5.2	2.0
14 TeV LHC	163	356	43	444	38	14	12	19	7.7

in Eq. (5) are mediated by virtual W ($\tilde{\nu}_\ell \bar{f}' f$), chargino ($\tilde{\nu}_\tau \nu_\ell \tau$, $\tilde{\tau}_1 \nu_\ell \nu_\tau$), or neutralino ($\tilde{\tau}_1 \ell \tau$, $\tilde{\nu}_\tau \ell \nu_\tau$) exchange. It is interesting to note that the decay mode $\tilde{\ell}_L \to \tilde{\nu}_\tau \ell \nu_\tau$ is highly suppressed because of a destructive interference between $\tilde{\chi}_1^0$ and $\tilde{\chi}_2^0$ exchange contributions. Similarly, for the electron-sneutrino we have only 3-body decays

$$\tilde{\nu}_\ell \to \tilde{\tau}_1 + \nu_\ell + \tau, \qquad \tilde{\tau}_1 + \ell + \nu_\tau, \qquad \tilde{\nu}_\tau + \nu_\ell + \nu_\tau, \qquad \tilde{\nu}_\tau + \ell + \tau. \tag{6}$$

These decays are mediated by virtual chargino ($\tilde{\tau}_1 \ell \nu_\tau$, $\tilde{\nu}_\tau \ell \tau$) or neutralino ($\tilde{\tau}_1 \nu_\ell \tau$, $\tilde{\nu}_\tau \ell \tau$) exchange. The decay width of the sneutrino is highly suppressed with respect to the left sleptons (see Table II). Heavier selectron mass provides more phase space, and the number of accessible decay modes is significantly larger. The stau $\tilde{\tau}_1$ can practically[4] decay only to the tau sneutrino $\tilde{\nu}_\tau$,

[4]Since the direct decay of stau to gravitino is negligible.

$$\tilde{\tau}_1 \to \tilde{\nu}_\tau + \bar{f}' + f, \qquad \tilde{\nu}_\tau^* + \nu_\tau + \tau^-, \tag{7}$$

where the dominant decay mode is mediated via W ($\tilde{\nu}_\tau \bar{f}' f$) and the other one by chargino and neutralino. We use SDECAY 1.3 [14] to calculate the 2-body decay branching ratios, and the FEYNARTS/FORMCALC [15] package to calculate the 3-body decay widths.[5] The branching ratios for the decay channels with branching ratios $\gtrsim 1\%$ are collected in Table II. Note that the dominant decay mode for $\tilde{\nu}_\ell$ is invisible.

We calculate the (pair) production rates for the sparticles in our model at the Tevatron and at the LHC. We assume three center-of-mass (c.m.) energies for the LHC: 7 TeV, 10 TeV, and 14 TeV. The results are shown in Table III. Note that the chargino ($\tilde{\chi}_1^\pm$) and neutralinos ($\tilde{\chi}_{1,2}^0$) are relatively heavy in our model and near the production threshold for the Tevatron. Note, also, that the squarks and gluinos are not produced at the Tevatron because of their heavy masses.

For the light sparticles' pair production processes, i.e., Table III(a) and (b), we see that at the Tevatron $\tilde{\nu}_\tau \tilde{\nu}_\tau^*$ (which is invisible) has the largest cross section due to the light $\tilde{\nu}_\tau$ mass, followed by $\tilde{\tau}_1^+ \tilde{\nu}_\tau$ and $\tilde{\tau}_1^- \tilde{\nu}_\tau^*$ (which are the largest visible channels). For the LHC, which is a proton-proton collider, $\tilde{\tau}_1^+ \tilde{\nu}_\tau$ has the largest cross section, followed by $\tilde{\nu}_\tau \tilde{\nu}_\tau^*$ and $\tilde{\tau}_1^- \tilde{\nu}_\tau^*$. For both colliders, gaugino production is subdominant due to their (relatively) heavy masses, and in the case of $\tilde{\chi}_1^0$, also by its bino-dominated content. As in most models with neutralino LSP (e.g., SPS1a [18]), $\tilde{\chi}_2^0 \tilde{\chi}_1^\pm$-associated production is the largest among the gauginos, followed by $\tilde{\chi}_1^- \tilde{\chi}_1^+$. For comparison, the $\tilde{\chi}_2^0 \tilde{\chi}_1^\pm$ production rates for SPS1a at the LHC is about 900 fb, for 14 TeV c.m. energy.

As we can see from the table, squarks and gluinos require large energy because of their heavy masses. At 7 TeV, the production of squarks and gluinos is negligibly small. At 10 TeV, their total production rate is still lower than that of sleptons. At 14 TeV, the $\tilde{g}\,\tilde{q}$ becomes important and, together with $\tilde{q}\,\tilde{q}$, provide promising channels for SUSY discovery.

III. THE LEPTONIC SIGNATURES

Let us now look at the supersymmetric signals in our model. First, let us focus on the pure multilepton plus missing energy signals without associated jet.[6] These signals are generated from the production of color singlet sparticles, i.e., the charginos, neutralinos, and sleptons. Thus, we look at chargino pair production ($\tilde{\chi}_1^\pm \tilde{\chi}_1^\mp$),[7] neutralino pair production ($\tilde{\chi}_i^0 \tilde{\chi}_j^0$), associated chargino-neutralino production ($\tilde{\chi}_1^\pm \tilde{\chi}_j^0$), and slepton pair production ($\tilde{\ell}_L'^+ \tilde{\ell}_L'^-$, $\tilde{\ell}_L'^- \tilde{\nu}_{\ell'}^*$, $\tilde{\ell}_L'^+ \tilde{\nu}_{\ell'}$ and $\tilde{\nu}_{\ell'}^* \tilde{\nu}_{\ell'}$, where $\ell' = e, \mu, \tau$) as listed in Table III. From here on, we will implicitly assume the case for the LHC at 14 TeV, unless explicitly stated otherwise.

Let us first look closer at the dominant leptonic decay modes for sleptons, sneutrinos, the lightest chargino, and the second-lightest neutralino. The charged sleptons of the first two generations can decay directly to $\tilde{\nu}_\tau$ as

$$\tilde{\ell}_L^- \to \tilde{\nu}_\tau^* + \tau^- + \nu_\ell, \qquad \tilde{\ell}_L^+ \to \tilde{\nu}_\tau + \tau^+ + \bar{\nu}_\ell. \tag{8}$$

Note that the decay channels $\tilde{\ell}^- \to \tilde{\nu}_\tau + \bar{\nu}_\tau + \ell^-$, $\tilde{\nu}_\tau^* + \nu_\tau + \ell^-$ are suppressed due to the cancellations mentioned below Eq. (5), in Sec. II. The selectron/smuon can also decay to the respective sneutrino

$$\tilde{\ell}_L^- \to \tilde{\nu}_\ell + \ell'^- + \bar{\nu}_{\ell'}, \qquad \tilde{\ell}_L^+ \to \tilde{\nu}_\ell^* + \ell'^+ + \nu_{\ell'}, \tag{9}$$

where again $\ell \equiv e, \mu$ and $\ell' \equiv e, \mu, \tau$; or with smaller branching ratios to the stau

$$\tilde{\ell}_L^\pm \to \tilde{\tau}_1^- + \tau^+ + \ell^\pm, \qquad \tilde{\tau}_1^+ + \tau^- + \ell^\pm. \tag{10}$$

The electron/muon-sneutrino decays mostly invisibly to the tau sneutrino and neutrinos. The largest visible decay mode is

$$\tilde{\nu}_\ell \to \ell^- + \tilde{\nu}_\tau + \tau^+, \qquad \tilde{\nu}_\ell^* \to \ell^+ + \tilde{\nu}_\tau^* + \tau^-. \tag{11}$$

They can also decay to stau:

$$\tilde{\nu}_\ell \to \tilde{\tau}_1^+ + \nu_\tau + \ell^-, \qquad \tilde{\nu}_\ell^* \to \tilde{\tau}_1^- + \bar{\nu}_\tau + \ell^+. \tag{12}$$

The leptonic decays of stau are

$$\tilde{\tau}_1^+ \to \tilde{\nu}_\tau^* + \ell'^+ + \nu_{\ell'}, \qquad \tilde{\tau}_1^- \to \tilde{\nu}_\tau + \ell'^- + \bar{\nu}_{\ell'}. \tag{13}$$

The second-lightest neutralino has a much larger production rate (in association with chargino) than the lightest neutralino, due to its mostly wino content. It decays as

$$\tilde{\chi}_2^0 \to \tilde{\ell}_L'^\mp + \ell'^\mp, \qquad \tilde{\nu}_{\ell'} + \bar{\nu}_{\ell'}, \qquad \tilde{\nu}_{\ell'}^* + \nu_{\ell'}. \tag{14}$$

The chargino decays as

$$\tilde{\chi}_1^+ \to \tilde{\nu}_{\ell'} + \ell'^+, \quad \tilde{\ell}_L'^+ + \nu_{\ell'}, \quad \tilde{\chi}_1^- \to \tilde{\nu}_\ell^* + \ell^-, \quad \tilde{\ell}_L'^- + \bar{\nu}_{\ell'}. \tag{15}$$

We can classify the pure leptonic signals based on the number of the isolated leptons (e, μ, and τ[8]) in the final state as follows:

(I) *1 lepton* + $\not{E}_T$: The signals can appear from:

(1) $\tilde{\tau}_1^- \tilde{\nu}_\tau^*$ ($\tilde{\tau}_1^+ \tilde{\nu}_\tau$) production with the stau decays to $\tilde{\nu}_\tau + \bar{\nu}_{\ell'} + \ell'$, where ℓ' could be either e, μ, or τ.

(2) $\tilde{\ell}_L^- \tilde{\nu}_\ell^*$ ($\tilde{\ell}_L^+ \tilde{\nu}_\ell$) production with the sneutrino decays invisibly as $\tilde{\nu}_\ell \to \tilde{\nu}_\tau + \nu_\ell + \nu_\tau$, while the selectron/smuon decays as $\tilde{\ell}_L^- \to \tilde{\nu}_\tau^* + \nu_\ell + \tau^-$.

[5] The 3-body decays of sleptons and sneutrinos have also been calculated analytically by Kraml and Nhung in [16].

[6] We will consider inclusive searches, including jets production, in Sec. IV.

[7] Same-sign chargino pairs can only be produced with some associated jets [19].

[8] We will consider tau decays in Sec. V.

Since the branching ratio for selectron/smuon decay to $\tilde{\nu}_\tau + \ell + \nu_\tau$ is small, the τ final state is dominant.

(3) $\tilde{\chi}_1^\pm \tilde{\chi}_2^0$ production with the chargino decays to $\tilde{\nu}_\tau + \tau$, and the neutralino decays to $\tilde{\nu}_\tau + \nu_\tau$. Again, the τ final state is dominant.

The SM backgrounds are coming from direct charged lepton + neutrino production through s-channel W boson exchange, from single W boson production with a cross section of 20 nb [20], and from WZ with invisible Z with a cross section 3.3 pb [21,22]. These backgrounds are, by orders of magnitude, larger than the SUSY signals, which are $O(10$ fb).

(II) *2 leptons + $\not{E}_T$ (dilepton)*: The SUSY signals can arise from

(1) $\tilde{\ell}_L^+ \tilde{\ell}_L^-$ production where each slepton produces one tau through 3-body decay $\tilde{\ell}_L \to \tilde{\nu}_\tau + \tau + \nu_\ell$.

(2) $\tilde{\tau}_1^+ \tilde{\tau}_1^-$ production with each stau decaying through 3-body decay mode $\tilde{\tau}_1 \to \tilde{\nu}_\tau + \nu_{\ell'} + \ell'$ where $\ell' = e, \mu, \tau$.

(3) $\tilde{\nu}_\ell \tilde{\nu}_\ell^*$ pair production with one of the sneutrinos decaying as $\tilde{\nu}_\ell \to \tilde{\nu}_\tau + \ell + \tau$, producing a tau and an electron/muon of opposite signs, while the other one decays invisibly as $\tilde{\nu}_\ell \to \tilde{\nu}_\tau + \nu_\ell + \nu_\tau$.

(4) $\tilde{\chi}_1^- \tilde{\chi}_1^+$ pair production with the charginos decaying to $\tau^- \tilde{\nu}_\tau^*$ and $\tau^+ \tilde{\nu}_\tau$, respectively.

Contributions from neutralino pair production is suppressed by the small production rate. The SM backgrounds come from direct production through γ^*, Z^* (Drell-Yan); from single Z boson production (with a cross section of 1.9 nb [20]); from ZZ, where one Z yields a neutrino-antineutrino pair, while the other Z yields $\ell'^+ \ell'^-$ (with a cross section of 0.3 pb [22,23]); and from W^+W^- production (with a cross section of 12.6 pb [24]). Again, the SM backgrounds are much larger than the SUSY signals.

(III) *3 leptons + $\not{E}_T$ (trilepton)*: The SUSY signals can come from

(1) $\tilde{\ell}_L^- \tilde{\nu}_\ell^*$ ($\tilde{\ell}_L^+ \tilde{\nu}_\ell$)-associated production, followed by $\tilde{\ell}_L^- \to \tilde{\nu}_\tau^* + \nu_\ell + \tau^-$ and $\tilde{\nu}_\ell^* \to \tilde{\nu}_\tau^* + \ell^+ + \tau^-$ decays. In this case, we have two taus of the same sign and an electron or a muon of the opposite sign.

(2) $\tilde{\chi}_1^\pm \tilde{\chi}_2^0$-associated production, with the chargino decays as $\tilde{\chi}_1^- \to \tau^- + \tilde{\nu}_\tau^*$ and the neutralino decays as (a) $\tilde{\chi}_2^0 \to \tilde{\ell}_L^\pm + \ell^\mp$ followed by $\tilde{\ell}_L \to \tilde{\nu}_\tau + \nu_\ell + \tau$, (b) $\tilde{\chi}_2^0 \to \tilde{\tau}_1^\pm + \tau^\mp$ followed by $\tilde{\tau}_1 \to \tilde{\nu}_\tau + \nu_{\ell'} + \ell'$, or (c) $\tilde{\chi}_2^0 \to \tilde{\nu}_\ell + \nu_\ell$ followed by $\tilde{\nu}_\ell \to \tilde{\nu}_\tau + \tau + \ell$.

The SM backgrounds for three leptons are from WZ and $W\gamma^*$.[9] For the neutralino LSP case, in which the dominant channel is through $\tilde{\chi}_1^\pm \tilde{\chi}_2^0$-associated production, this trilepton signature has been studied thoroughly and appears to be a promising channel to discover SUSY [26]. In our scenario, however, the $\tilde{\chi}_1^\pm \tilde{\chi}_2^0$ production is subdominant (and certainly insufficient for the Tevatron), and the trilepton signals come mostly from $\tilde{\ell}_L^+ \tilde{\nu}_\ell$ and $\tilde{\ell}_L^- \tilde{\nu}_\ell^*$ production. It is interesting to notice, however, that for our scenario, we can have two taus of the same sign (i.e., SF + SS), and that the SM background for this is expected to be smaller. In this case, the SM background receives contributions from the production of three W bosons, which has a small cross section.

(IV) *4 leptons + $\not{E}_T$*: The SUSY signals can arise from

(1) $\tilde{\nu}_\ell \tilde{\nu}_\ell^*$ production, followed by $\tilde{\nu}_\ell \to \tilde{\nu}_\tau + \tau + \ell$ decays.

(2) $\tilde{\ell}_L^+ \tilde{\ell}_L^-$ production, with one $\tilde{\ell}_L$ decaying as $\tilde{\ell}_L^- \to \tilde{\nu}_\ell + \ell'^- + \bar{\nu}_{\ell'}$ (where $\ell' \equiv e, \mu, \tau$) followed by $\tilde{\nu}_\ell \to \tilde{\nu}_\tau + \ell^- + \tau^+$, while the other slepton decays as $\tilde{\ell}_L^+ \to \tilde{\nu}_\tau + \tau^+ + \bar{\nu}_\ell$.

(3) $\tilde{\chi}_1^+ \tilde{\chi}_1^-$ production, with one of the charginos decaying as $\tilde{\chi}_1^- \to \tilde{\nu}_\tau^* + \tau^-$ and the other one decaying through $\tilde{\chi}_1^+ \to \tilde{\nu}_\ell + \ell^+$ followed by $\tilde{\nu}_\ell \to \tilde{\nu}_\tau + \tau^+ + \ell^-$.

The dominant SM background comes from ZZ that has a cross section of 0.12 pb [23]. In our scenario, Higgs bosons H and A are quite heavy (~ 2 TeV); therefore, their production at the LHC would be suppressed. Moreover, the neutralinos and charginos in our scenario are also relatively heavy. Thus, we do not consider the same kind of analysis as done in [27].

(V) *5 leptons + $\not{E}_T$*: The SUSY signals can arise from

(1) $\tilde{\ell}_L^+ \tilde{\nu}_\ell$ ($\tilde{\ell}_L^- \tilde{\nu}_\ell^*$)-associated production, where the $\tilde{\ell}_L$ decays similarly as in the 4-leptons case, producing 3 leptons while the sneutrino decays as $\tilde{\nu}_\ell \to \tilde{\nu}_\tau + \ell + \tau$.

(2) Again, neutralino-chargino $\tilde{\chi}_2^0 \tilde{\chi}_1^\pm$-associated production provides subdominant contribution. Here, the neutralino decays as $\tilde{\chi}_2^0 \to \tilde{\ell}' + \ell'$, followed by $\tilde{\ell}' \to \tilde{\nu}_\tau + \tau + \nu_{\ell'}$,[10] while the chargino decays as $\tilde{\chi}_1^\pm \to \tilde{\nu}_\ell + \ell$, followed by $\tilde{\nu}_\ell \to \tilde{\nu}_\tau + \ell + \tau$.

The SM backgrounds are from WZZ [28], $WZ\gamma^*$, and $W\gamma^*\gamma^*$. Note that even though the SUSY 5-lepton signal has a small rate $O(0.1$ fb), suppressed by branching ratios of $\tilde{\ell}_L$ and $\tilde{\nu}_\ell$ decays, the SM background is also small. Thus, this might also be an interesting channel to look at. The question, however, is how much luminosity would be needed to receive enough significance.

[9] At the detector level, there are also some processes that can mimic trilepton signature, such as ZZ, $t\bar{t}$, Drell-Yan, and fake leptons [25].

[10] Recall that for this specific model, the decay $\tilde{\ell}' \to \tilde{\nu}_\tau + \ell + \nu_\tau$ has a very small branching ratio. Having this decay channel available, we would have 5-lepton signature with only one tau.

IV. THE TRILEPTON SIGNALS AND BACKGROUNDS

As mentioned in Sec. III, the trilepton signature with a pair of like-sign taus is particularly interesting. The signals that we are looking for are $\tau^+\tau^+(e,\mu)^-$ and $\tau^-\tau^-(e,\mu)^+$, which, in our SUSY scenario, arise mainly from slepton-sneutrino-associated production followed by cascade decays (illustrated in Fig. 1). If the taus and their charges could be identified in the detectors, then this would provide us with an excellent supersymmetric signal with a distinctly larger cross section than the SM background. In the SM, this signature can be mimicked, primarily through the production and decay of three W bosons:

$$pp \to W^+W^+W^- \to \tau^+\nu_\tau\tau^+\nu_\tau\ell^-\bar{\nu}_\ell, \tag{16}$$

and

$$pp \to W^-W^-W^+ \to \tau^-\bar{\nu}_\tau\tau^-\bar{\nu}_\tau\ell^+\nu_\ell, \tag{17}$$

respectively.

In reality, however, taus decay quickly inside the detectors, producing either leptons (i.e., e, μ and neutrinos) or jets (plus tau neutrino). Tau identification could present a problem, especially for a hadron collider such as the LHC with high jet multiplicities. If a tau decayed to e/μ, then it would be difficult to distinguish it from the electrons/muons produced by other processes. On the other hand, it is not easy—although not impossible—to identify jets that are coming from taus [29,30]. Let us recapitulate on the signals as seen by the detectors:

(a) $e^\pm\mu^\pm(e,\mu)^\mp$,
(b) $e^\pm e^\pm e^\mp$, $\mu^\pm\mu^\pm\mu^\mp$,
(c) $e^\pm e^\pm\mu^\mp$, $\mu^\pm\mu^\pm e^\mp$,
(d) $\tau_h^\pm(e^\pm\mu^\mp, \mu^\pm e^\mp)$,
(e) $\tau_h^\pm(e^\pm e^\mp, \mu^\pm\mu^\mp)$,
(f) $\tau_h^\pm\tau_h^\pm(e,\mu)^\mp$.

Here, τ_h represents a hadronic tau. The ratios are approximately

$$(a):(b):(c):(d):(e):(f) \simeq 6:3:3:22:22:42. \tag{18}$$

At this level, there is another SM background from the following process:

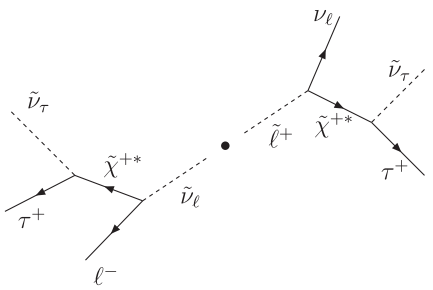

FIG. 1. Example of trilepton signature from slepton-sneutrino-associated production.

$$pp \to W^+Z \to \tau^+\tau^+\tau^-\nu_\tau, \tag{19}$$

with the taus decaying either leptonically or hadronically. In addition, there is a background from WWW, which can produce the leptonic signals directly without going through any tau. Signals (a), (b), and (e) also receive backgrounds from WZ and $W\gamma^*$, which produce e/μ directly. Thus, the interesting signals to look at are (c), (d), and (f). Signal (c) provides a clear signature, but is suppressed by the branching ratios. Although (d) is quite interesting, the signals might be overwhelmed by fake taus. Therefore, we concentrate on (f) in our analysis, where we look for two tau jets of the same sign and a muon/electron of the opposite sign. From here on, we will always mean hadronic tau (τ_h) when we say tau (τ), unless explicitly stated otherwise.

At the simulation level, we need to consider some additional backgrounds. This is due to the fact that there could be some leptons or jets that do not pass the selection criteria, resulting in a different signature. For example, we can have ZZ with each Z decaying to a pair of taus, then two taus decaying hadronically, one tau leptonically while the other one is missing. Thus, for $\tau^+\tau^+\mu^-$ signal, we need to include Z-pair, top-pair, and single-top W-associated production as well.

The detection of hadronic tau is also not straightforward. Full analysis would require detector simulation and tau reconstruction, which are beyond the scope of our paper. To take the tau identification problem into account, we can make an estimate by attaching a detection efficiency factor to each hadronic tau, $0 < \epsilon_h < 1$. However, to be more precise, this factor should be taken as a function of transverse momentum and pseudorapidity [31,32]. Note that this factor affects both the signal and the background. For this reason, we do not include this factor in the histograms shown in Sec. V. In addition, the tau charge should also be identified correctly for our case. Charge identification is expected to become worse for larger tau momentum, although it should not be impossible for the interesting range in our model at the LHC [29]. This charge identification can be used to eliminate some background events arising from $t\bar{t}$, but not entirely.

At the detector level, there could be additional backgrounds from jets that are misidentified as taus, i.e., fake tau signals. For example, the Wjj, which has a much larger production rate [33], can be problematic. The rejection rate of fake taus depends on the detector's capability and is correlated to the tau identification efficiency [29]. If we assume an (effective) rejection factor of 500, with an $e^+\nu_e jj$ cross section of 670 pb, we obtain 2.4 fb of fake tau background, which is comparable to the SUSY signal. We notice that the missing transverse energy for this background is below 200 GeV.

On the other hand, hadron colliders, such as the LHC, produce many jets in both SUSY and SM processes.

By looking at trileptons plus any number of jets, we would obtain more signal events. We start with an inclusive search of $\tau^{\pm}\tau^{\pm}\mu^{\mp} + nj$, where $n = 0, 1, 2, \ldots$, and then employ cuts to reduce the backgrounds. Our SUSY signal now consists of slepton-sneutrino, chargino-neutralino, and SUSY QCD. In SUSY QCD, squarks and gluinos are produced and cascade decay to the tau-sneutrino NLSP. We found that this SUSY QCD contribution gives large transverse energy to the final states, due to the big gap between the squark sector and the slepton sector in our model. Thus, this can be used as initial evidence of new physics beyond the SM.

V. ANALYSIS AND RESULTS AT THE LHC

In this section, we study the inclusive trilepton signals at the LHC for a c.m. energy of 14 TeV. The inclusive SUSY signal has been generated by the Monte Carlo program HERWIG++ 2.4.2 [17]. We have included all sparticle pair production processes and all possible 2-body and 3-body sparticle decays in the HERWIG++ simulations. All background processes have been simulated with the Monte Carlo program SHERPA 1.2.0 [34]. For the SHERPA simulations, we have used COMIX [35] to compute the hard matrix elements.

After generating events, we apply the following selection criteria:

(1) Jets reconstructed according to the anti-k_T algorithm with $D = 0.7$ [36], which are required to have

$$p_T^j > 20 \text{ GeV}, \qquad |\eta_j| < 4.5. \tag{20}$$

(2) $N_\mu = 1$: Isolated muons with $R_{\mu,j} > 0.7$.

(3) $N_\tau = 2$: Isolated like-sign taus with $R_{\tau,j} > 0.7$.

(4) The hardest lepton is required to have

$$p_T^\ell > 10 \text{ GeV}, \qquad |\eta_\ell| < 2.5. \tag{21}$$

(5) The two hardest taus in the event are required to have

$$p_T^{\tau_h} > 15 \text{ GeV}, \qquad |\eta_{\tau_h}| < 2.5. \tag{22}$$

(6) Leptons and taus are required to be isolated with

$$R_{\ell,\tau_h} > 0.4 \qquad R_{\tau_h,\tau_h} > 0.4. \tag{23}$$

These form our basic cuts. We have used RIVET 1.2.1 [37] and FASTJET 2.4.2 [38] in order to analyze events according to our prescribed selection criteria.

In Fig. 2, we show the transverse momentum distribution for the hardest jet, p_T^{j1}, after the basic cuts. It is obvious that the distribution at large p_T is dominated by contributions from SUSY QCD, i.e., from production of squarks and gluinos—similarly for the second-, third-, and fourth-hardest jets. This would provide a clear signal of new physics beyond the SM. Note that this feature should also be found for signals with any number of leptons in our scenario, and also for other scenarios in which squarks and gluinos are much heavier than the LSP. Thus, although high p_T jets indicate new physics, it is not a unique feature of our model.

We then apply optimized cuts to enhance the signal-to-background ratio. At this point, we have two branches of analysis. The main branch is focusing on the leptonic features of the SUSY signal, with the following set of cuts:

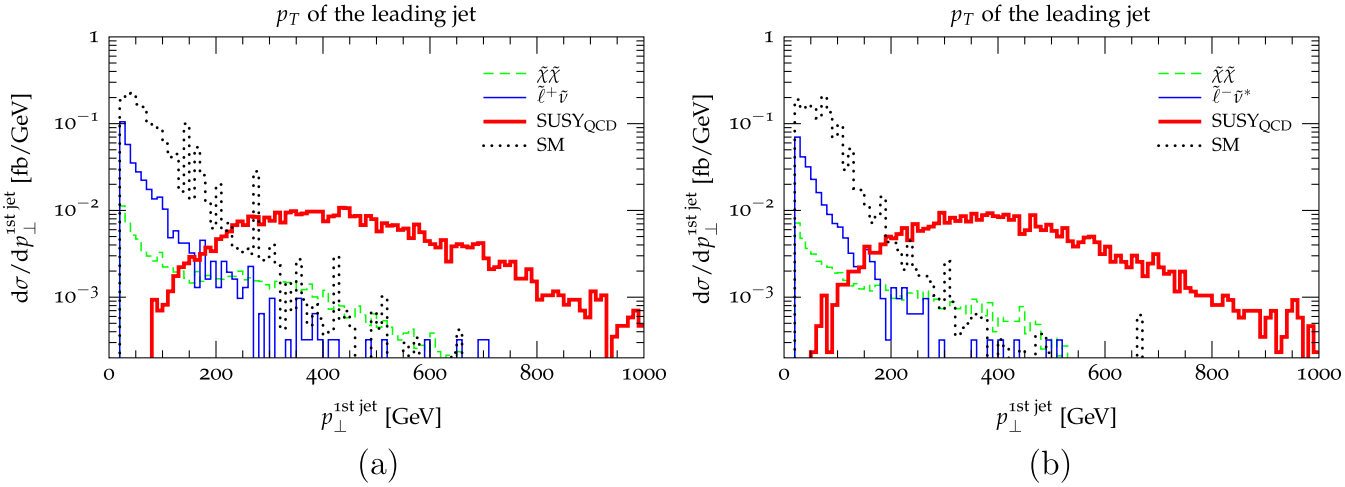

FIG. 2 (color online). The distribution of the hardest jet transverse momentum, $p_T^{\rm j1}$ for (a) $\tau^+\tau^+\mu^-$ + jets and (b) $\tau^-\tau^-\mu^+$ + jets for SUSY signals and SM background.

(I)

(1) Veto on b jets and more than one jet, i.e., $N_b = 0$ and $N_j \leq 1$.

(2) Cut on the transverse momentum of the hardest jet in the event above 200 GeV: i.e., we require $20\ \text{GeV} < p_T^{j1} \leq 200\ \text{GeV}$.

(3) Require $m_{\min}(\mu, \tau) = \min(m(\mu_1, \tau_1), m(\mu_1, \tau_2)) < 55$ GeV and $\phi(\mu, \not{p}_T) \geq 1.5$ rads.

We call this set opt.A for short. It optimizes the SUSY EW signal. For the side branch analysis, we have the following set of cuts (opt.B) which is designed to promote the high-p_T jet of the SUSY QCD signal [39,40]:

(II)

(1) We require $N_j \geq 2$ and $p_T^{j1} \geq 200$ GeV, and

(2) $A_T' = \sum_{i=\text{leptons,jets}} E_T^i \geq 300$ GeV.

The results of our simulations are tabulated in Table IV for the $\ell = \mu$ case. The $\ell = e$ case is similar to the μ case, hence is not shown here. Backgrounds for the case of the $\tau^+\tau^+\ell^-$ signature include $\tau^+\nu_\tau\tau^+\nu_\tau\mu^-\bar{\nu}_\mu$ denoted simply as $W^+W^+W^-$, $\tau^+\tau^-\tau^+\nu_\tau$ denoted as ZW^+, $\tau^+\tau^-\tau^+\tau^-$ denoted as ZZ, $W^+[\to \tau^+\nu_\tau]W^-[\to \mu^-\bar{\nu}_\mu]b\bar{b}\tau^+\tau^-$ denoted as $t\bar{t}Z$, $t[\to b\tau^+\nu_\tau]\bar{t}[\to \bar{b}\mu^-\nu_\mu]W^+[\to \tau^+\nu_\tau]$ denoted as $t\bar{t}W^+$, $W^+[\to \tau^+\nu_\tau]W^-[\to \mu^-\overline{\nu}_\mu]b\bar{b}$ denoted as $W^+W^-b\bar{b}$, and $\mu^-\bar{\nu}_\mu\tau^+\nu_\tau\tau^+\tau^-$ denoted as ZW^+W^-. Note that the backgrounds from top-pair production and single-top W boson–associated production are already included in $W^+W^-b\bar{b}$. We have similar backgrounds for the $\tau^-\tau^-\ell^+$, but with the charges conjugated.

TABLE IV. Generation characteristics for $pp \to \mu^-\tau_h^+\tau_h^+ + E_T$ and $pp \to \mu^+\tau_h^-\tau_h^- + E_T$. Tau detection efficiency is not included.

$\tau^+\tau^+\mu^-$	σ_{basic} [fb]	σ_{optA} [fb]	σ_{optB} [fb]
Susy EW	3.55	1.78	0.0828
Susy QCD	4.09	0.00	3.73
Susy $\chi\chi$	1.83	0.0986	0.322
ZW^+	4.80	0.829	0.200
ZZ	1.80	0.172	0.0164
$W^+W^-b\bar{b}$	10.4	0.0390	0.285
$t\bar{t}W^+$	0.0506	5.81×10^{-5}	0.002 89
$t\bar{t}Z$	0.127	3.50×10^{-5}	0.006 42
$W^+W^+W^-$	0.0728	0.0117	0.004 23
ZW^+W^-	0.0348	0.004 53	0.002 32
$\tau^-\tau^-\mu^+$	σ_{basic} [fb]	σ_{optA} [fb]	σ_{optB} [fb]
Susy EW	2.46	1.24	0.0523
Susy QCD	3.51	0.001 50	3.18
Susy $\chi\chi$	0.676	0.0676	0.203
ZW^-	3.64	0.633	0.0927
ZZ	1.78	0.161	0.0161
$W^+W^-b\bar{b}$	9.07	0.0204	0.0529
$t\bar{t}W^-$	0.0305	5.02×10^{-5}	0.001 37
$t\bar{t}Z$	0.135	5.36×10^{-5}	0.005 71
$W^+W^-W^-$	0.0498	0.0106	0.002 99
ZW^+W^-	0.0333	0.004 80	0.002 36

In opt.A, the veto on jets helps to reduce the SM QCD background, in particular $t\bar{t}$, although it also suppresses the SUSY QCD signal. The cuts on $m_{\min}(\mu, \tau)$ and $\phi(\mu, \not{p}_T)$ are used to suppress backgrounds from ZZ and ZW. As we can see from the table, the SUSY signal is now comparable to the SM background. In total, it is greater than the background for both the $\tau^+\tau^+\mu^-$ and $\tau^-\tau^-\mu^+$ cases, but we obtain an improved result for the $\tau^+\tau^+\mu^-$ case. With opt.B, on the other hand, the SUSY EW signal is suppressed due to the low jet multiplicity. We see that after the optimization, we obtain a SUSY QCD signal significantly higher than the backgrounds.

We now focus our discussion on the main analysis (i.e., opt.A). In Fig. 3, we show the muon transverse momentum distribution p_T^μ after the optimized cuts. The largest background comes from ZW. The shape of ZW is following that of SUSY EW, but it is softer. However, the signal distribution is larger for smaller p_T^μ, decreasing rapidly with increasing p_T^μ. Therefore, there is less incentive to optimize the cut on p_T^μ.

The transverse momentum distributions of the two taus are shown in Fig. 4. Here, τ_1 is the hardest tau and τ_2 is the softer tau. The hardest tau momentum peaks at around 40 GeV, and the $p_T^{\tau_1}$ cut (in the basic cuts) does not reduce the signal much. For the softer tau, however, the cut is significant. Increasing the $p_T^{\tau_2}$ cut from 10 GeV to 30 GeV, for example, can reduce the effective cross section by $\sim$40%. We choose our cut at 15 GeV, which, although difficult from an experimental point of view, should be possible at the LHC. Again, we see that it is difficult to reduce the ZW background any further.

Figure 5 shows the distribution in the invariant mass of the μ and τ pair. We note that the signal distribution is concentrated at $m_{\tau\mu} < 50$ GeV. This suggests a bump feature which arises from the μ and τ pair, coming from the same decay chain [i.e., from $\tilde{\nu}_\mu$; see Eq. (6)]. The end point of this bump indicates a mass gap of $\sim$50 GeV between $\tilde{\nu}_\mu$ and $\tilde{\nu}_\tau$, which agrees with our mass spectrum. There is also a smooth distribution without an end point for high invariant masses. This arises from pairing the μ with the τ that comes from smuon decay. We might be able to cut ZW a little bit more in this case by cutting out around 60 GeV, but the gain is not significant.

In Fig. 6, we show the invariant mass distribution of the $\tau\tau$ pair. There is no end point feature seen in this plot, suggesting that the two taus always come from opposite decay chains. On the other hand, notice that the invariant mass distribution peaks at around 50 GeV, indicating that both taus are coming from decays of weak scale particles.

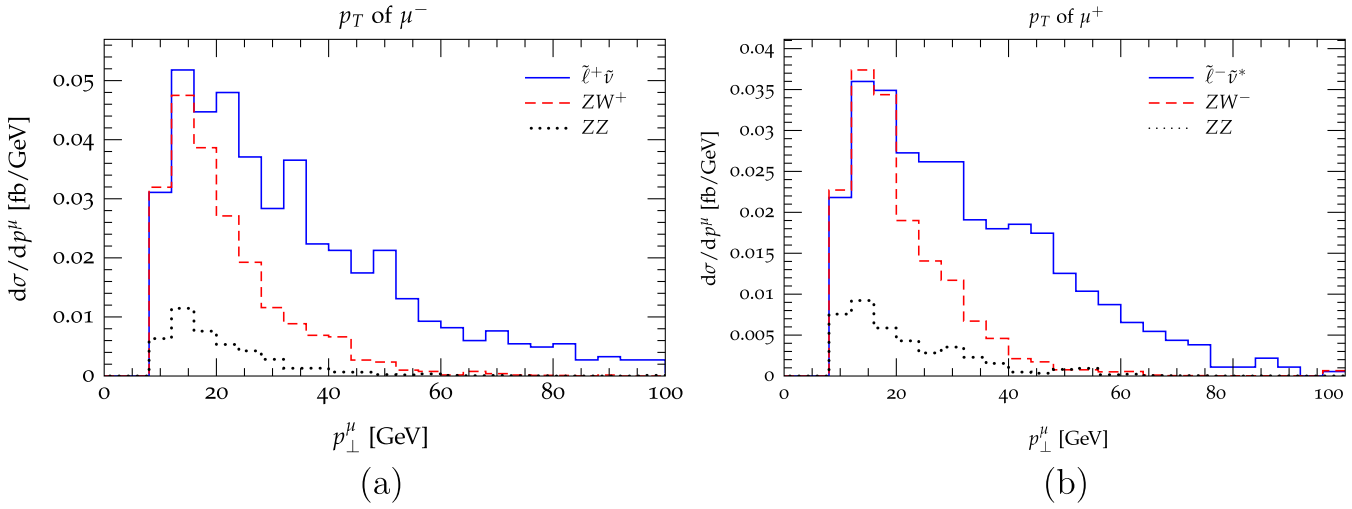

FIG. 3 (color online). The distribution in the (a) μ^- and (b) μ^+ transverse momenta, $p_T^{\mu^-}$ and $p_T^{\mu^+}$, respectively. Channels providing negligible contribution are not shown here.

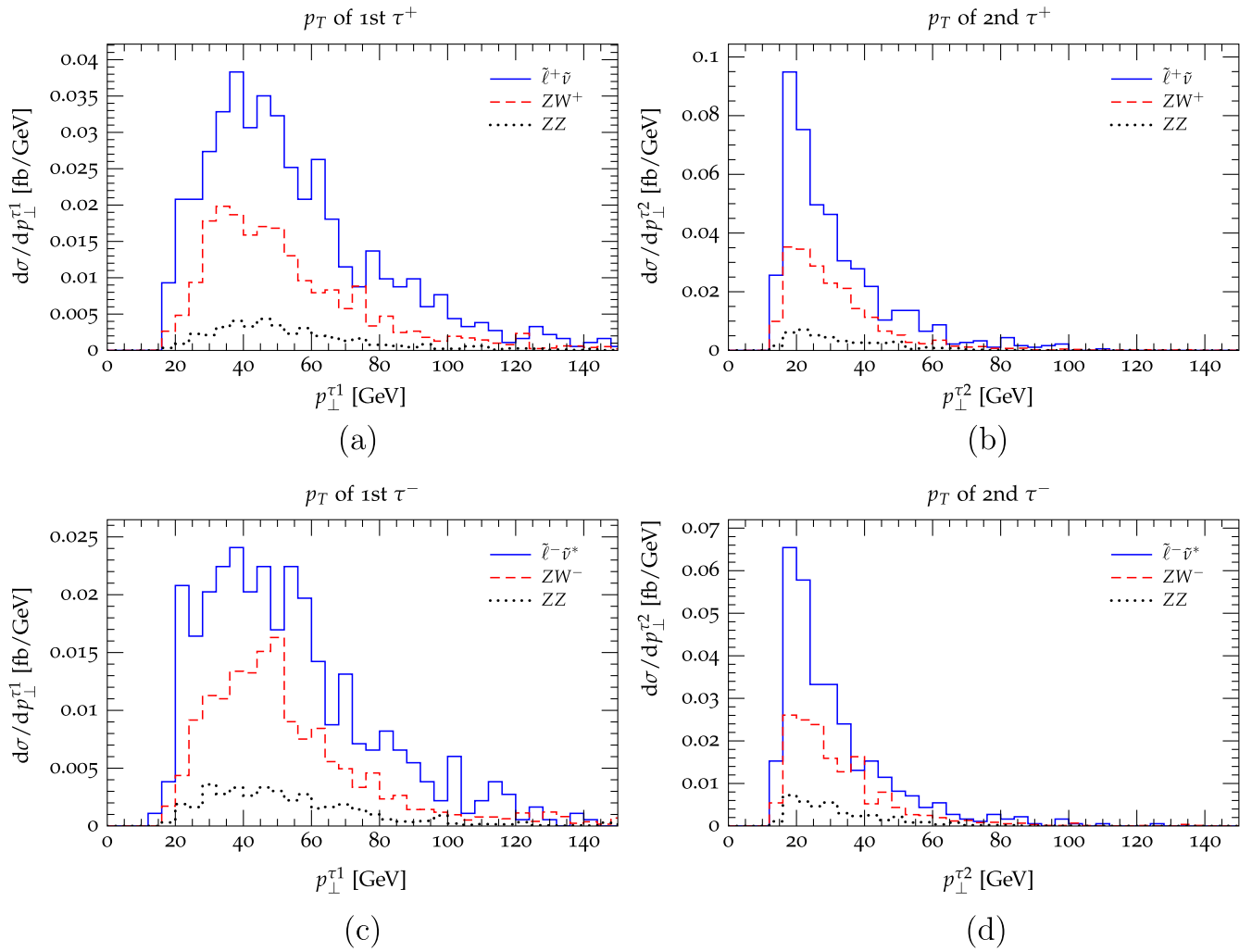

FIG. 4 (color online). The distribution in the (a, b) τ^+ and (c, d) τ^- transverse momenta, $p_T^{\tau^+}$ and $p_T^{\tau^-}$, respectively. Channels providing negligible contribution are not shown here.

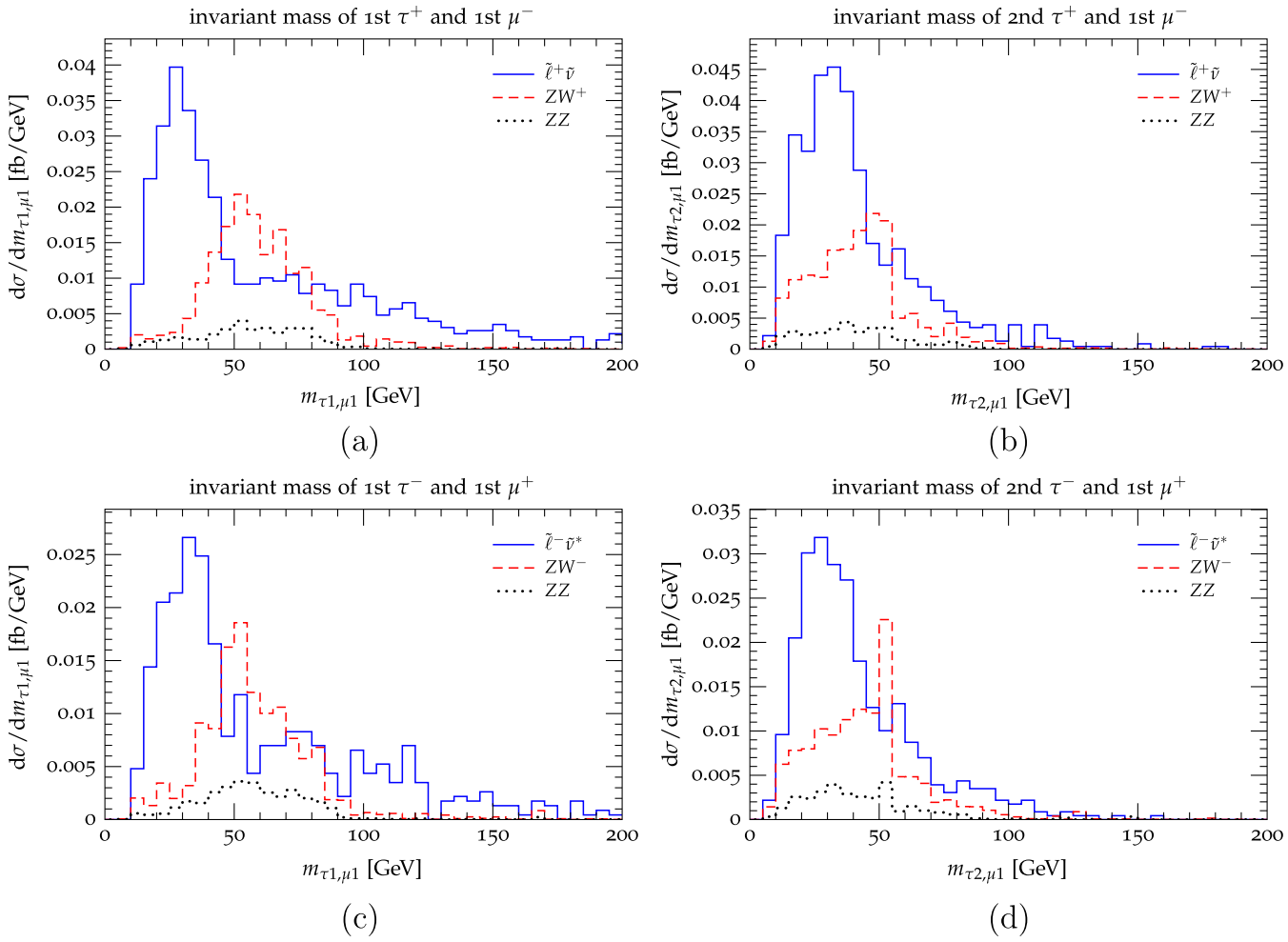

FIG. 5 (color online). The distribution in the (a, b) $\mu^-\tau^+$ and (c, d) $\mu^+\tau^-$ invariant masses. Here, τ_1 is the hardest tau, and τ_2 is the second-hardest. Channels providing negligible contribution are not shown here.

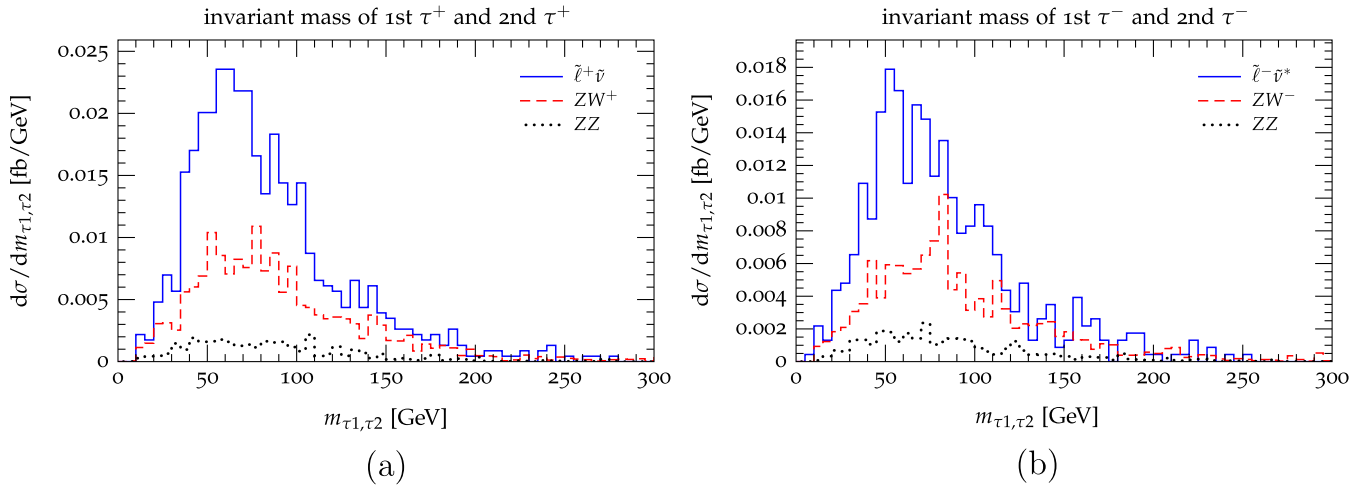

FIG. 6 (color online). The distribution in the (a) $\tau^+\tau^+$ and (b) $\tau^-\tau^-$ invariant masses. Channels providing negligible contribution are not shown here.

In all of the plots above, the tau efficiency factor ϵ has not been included. Note that since both signal and background are affected by ϵ, including this factor would only rescale the distribution height but would not change the ratio between signal and background,[11] except for the fake tau rate, which is not included in the plots. Here, we assume that the fake tau rate, which depends on the real data analysis, can be kept under control.

Significance can be estimated as follows:

$$\frac{S}{\sqrt{S+B}} = \frac{\sigma_S}{\sqrt{\sigma_S+\sigma_B}} \cdot \epsilon_{\rm eff} \cdot \sqrt{\int \mathcal{L}}, \tag{24}$$

where $\epsilon_{\rm eff}$ is the effective tau identification efficiency factor over the whole spectrum and $\int \mathcal{L}$ is an integrated luminosity. Here, we have used the fact that there are two taus in our signal, and assumed (for simplicity) the same effective efficiency factor $\epsilon_{\rm eff}$ for both taus. The tau charge identification efficiency is implicitly included in $\epsilon_{\rm eff}$, i.e., $\epsilon \equiv \epsilon_\tau \epsilon_{\rm charge}$.

Recalling the effective cross sections for the $\tau_h\tau_h\ell$ signal after the cuts as summarized in Table IV, we find that the total effective cross sections are $\sigma_{\rm opt.A}({\rm SUSY}) \simeq 3.2$ fb and $\sigma_{\rm opt.A}({\rm SM}) \simeq 1.9$ fb, respectively, including both $\tau^+\tau^+\mu^-$ and $\tau^-\tau^-\mu^+$. We see that for $5-\sigma$ discovery level, the required integrated luminosity is

$$\int \mathcal{L}(5\sigma)_{\rm opt.A} \simeq 12.5/\epsilon_{\rm eff}^2 \ ({\rm fb}^{-1}). \tag{25}$$

Taking $\epsilon_{\rm eff} = 0.4$ [29], for example, we find that $5-\sigma$ discovery requires about 80 fb^{-1} of data.

On the other hand, for p_T^j analysis (opt.B), we have $\sigma_{\rm opt.B}({\rm SUSY}) \simeq 7.6$ fb and $\sigma_{\rm opt.B}({\rm SM}) \simeq 0.7$ fb respectively, leading to

$$\int \mathcal{L}(5\sigma)_{\rm opt.B} \simeq 3.6/\epsilon_{\rm eff}^2 ({\rm fb}^{-1}). \tag{26}$$

Thus, with $\epsilon_{\rm eff} = 0.4$, $5-\sigma$ level in this case requires only about 23 fb^{-1} of data. Note that this is not necessarily the most promising channel to look for high p_T jets, i.e., we should also compare it with the pure jets channel, etc., each of which requires a separate set of analysis.

Here, we have assumed 14 TeV c.m. energy for our analysis. Even using the highest energy expected at the LHC, we see that we need a significant amount of data for discovery. We can deduce from Table III that it would be very difficult with 10 TeV c.m. energy and practically impossible with 7 TeV. Thus, we hope that the LHC can overcome its technical difficulties and reach the original designed energy of 14 TeV.

[11]Note, however, that ϵ varies with respect to some observables such as the tau transverse momentum p_T^τ and rapidity. Therefore, the rescaling is not constant.

VI. CONCLUSION

We have studied the leptonic signatures of a model in which the tau sneutrino is the effectively stable lightest supersymmetric particle at the LHC. The model that we consider has relatively heavy charginos and neutralinos, and relatively light sleptons and sneutrinos. The cross sections for pure leptonic signals are generally small, partly due to the fact that neutralino-chargino-associated production in this model is suppressed by the heavy gaugino masses. Nevertheless, we find that the trilepton signature is still interesting to look at. It consists of a signal with two like-sign taus and one electron or muon of the opposite sign, coming from $\tilde{\ell}_L\tilde{\nu}_\ell$ production.

We employ an inclusive search strategy in generating signals and use a set of cuts to look at this particular signature. At the Tevatron, the sparticle production rates are too small to yield any observable supersymmetric signal in our scenario. At the LHC, sufficiently large c.m. energy is still required. With 14 TeV and the optimized cuts, we can obtain $5-\sigma$ SUSY trilepton signals after $\sim$80 fb^{-1} integrated luminosity. We also investigated the leptons + jets signatures, and noticed that we can use a p_T^j cut to observe the new physics signal above the SM background. In our case, for $p_T^{j_1} \gtrsim 200$ GeV, where j_1 is the hardest jet, SUSY QCD is dominant due to the large mass gap between the squark sector and the slepton sector. In this way, we can obtain a significant signal-to-background ratio after 23 fb^{-1} of integrated luminosity. However, this does not tell us much about the underlying model, since this is generally true for any supersymmetric model with heavy squarks and gluinos. Note that these are optimistic estimates, assuming that we can suppress the fake tau event rate.

Our study suggests that the search for supersymmetry can be quite challenging, depending on the specific supersymmetric model. This is especially true when we want to look into the detailed characteristics of the model. Even though the slepton spectrum is relatively light—around 100 GeV—we still need large amount of data and high energy to see a significant excess of signal over background.

If this scenario is realized in nature, a big challenge in the data analysis at the LHC would come from tau reconstruction and identification, as well as rejection of fake taus. As tau can appear copiously in many models beyond SM, we might need new methods in this aspect. Indeed, there are ongoing efforts to alleviate these problems [41]. Nevertheless, hadron colliders, such as the LHC, might not be sufficient to explore the physics beyond the SM. In this case, a lepton collider such as the proposed e^+e^- International Linear Collider (ILC) [42] would help. For the ILC, the tau signal would be much cleaner. Only then would it be possible to probe the model further—for example, by reconstructing masses and measuring couplings.

ACKNOWLEDGMENTS

We received a lot of feedback during this project. Our special thanks go to Frank Krauss for many invaluable suggestions. We also thank Steffen Schumann, Tanju Gleisberg, David Grellscheid, Teruki Kamon, Bhaskar Dutta, Ayres Freitas, Gudrid Moortgat-Pick, Peter Richardson, Andy Buckley, Alice Bean, and Graham Wilson for various information and useful discussions. The work of Y. S. was supported in part by the DOE grant DE-FG02-04ER41308. K. R. is supported by the EU Network MRTN-CT-2006-035505 ''Tools and Precision Calculations for Physics Discoveries at Colliders'' (HEP-Tools).

[1] G. Weiglein *et al.* (LHC/LC Study Group), Phys. Rep. **426**, 47 (2006).
[2] J. Ellis, J. S. Hagelin, D. V. Nanopoulos, K. A. Olive, and M. Srednicki, Nucl. Phys. **B238**, 453 (1984); H. Goldberg, Phys. Rev. Lett. **50**, 1419 (1983).
[3] J. R. Ellis, K. A. Olive, Y. Santoso, and V. C. Spanos, Phys. Lett. B **588**, 7 (2004).
[4] J. L. Feng, S. Su, and F. Takayama, Phys. Rev. D **70**, 075019 (2004); **70**, 063514 (2004).
[5] L. Covi and S. Kraml, J. High Energy Phys. 08 (2007) 015.
[6] A. Katz and B. Tweedie, Phys. Rev. D **81**, 035012 (2010); **81**, 115003 (2010).
[7] H. Baer, C. H. Chen, F. Paige, and X. Tata, Phys. Rev. D **52**, 2746 (1995).
[8] H. Baer, C. H. Chen, F. Paige, and X. Tata, Phys. Rev. D **53**, 6241 (1996).
[9] J. R. Ellis, K. A. Olive, and Y. Santoso, Phys. Lett. B **539**, 107 (2002); J. R. Ellis, T. Falk, K. A. Olive, and Y. Santoso, Nucl. Phys. **B652**, 259 (2003).
[10] J. R. Ellis, K. A. Olive, and Y. Santoso, J. High Energy Phys. 10 (2008) 005.
[11] Tevatron Electroweak Working Group, CDF, and D0 Collaborations, arXiv:0808.1089.
[12] S. Heinemeyer, W. Hollik, and G. Weiglein, Comput. Phys. Commun. **124**, 76 (2000); S. Heinemeyer, W. Hollik, and G. Weiglein, Eur. Phys. J. C **9**, 343 (1999).
[13] S. Ambrosanio and B. Mele, Phys. Rev. D **53**, 2541 (1996).
[14] M. Muhlleitner, A. Djouadi, and Y. Mambrini, Comput. Phys. Commun. **168**, 46 (2005).
[15] J. Küblbeck, M. Bohm, and A. Denner, Comput. Phys. Commun. **60**, 165 (1990); T. Hahn, Comput. Phys. Commun. **140**, 418 (2001); T. Hahn and M. Perez-Victoria, Comput. Phys. Commun. **118**, 153 (1999); J. A. M. Vermaseren, arXiv:math-ph/0010025; T. Hahn and C. Schappacher, Comput. Phys. Commun. **143**, 54 (2002).
[16] S. Kraml and D. T. Nhung, J. High Energy Phys. 02 (2008) 061.
[17] M. Bahr *et al.*, Eur. Phys. J. C **58**, 639 (2008).
[18] B. C. Allanach *et al.*, Eur. Phys. J. C **25**, 113 (2002).
[19] J. Allwall, D. Rainwater, and T. Plehn, Phys. Rev. D **76**, 055006 (2007).
[20] A. D. Martin, R. G. Roberts, W. J. Stirling, and R. S. Thorne, Eur. Phys. J. C **14**, 133 (2000).
[21] S. Frixione, P. Nason, and G. Ridolfi, Nucl. Phys. **B383**, 3 (1992).
[22] J. M. Campbell and R. K. Ellis, Phys. Rev. D **60**, 113006 (1999).
[23] B. Mele, P. Nason, and G. Ridolfi, Nucl. Phys. **B357**, 409 (1991); L. J. Dixon, Z. Kunszt, and A. Signer, Phys. Rev. D **60**, 114037 (1999).
[24] S. Frixione, Nucl. Phys. **B410**, 280 (1993); T. Binoth, M. Ciccolini, N. Kauer, and M. Kramer, J. High Energy Phys. 12 (2006) 046.
[25] T. Aaltonen *et al.* (CDF Collaboration), Phys. Rev. Lett. **101**, 251801 (2008).
[26] H. Baer, C. H. Chen, F. Paige, and X. Tata, Phys. Rev. D **50**, 4508 (1994); V. D. Barger, C. Kao, and T. J. Li, Phys. Lett. B **433**, 328 (1998); V. D. Barger and C. Kao, Phys. Rev. D **60**, 115015 (1999); H. Baer, M. Drees, F. Paige, P. Quintana, and X. Tata, Phys. Rev. D **61**, 095007 (2000); E. Accomando, R. L. Arnowitt, and B. Dutta, Phys. Lett. B **475**, 176 (2000); Z. Sullivan and E. L. Berger, Phys. Rev. D **78**, 034030 (2008).
[27] G. Bian, M. Bisset, N. Kersting, Y. Liu, and X. Wang, Eur. Phys. J. C **53**, 429 (2008); P. Huang, N. Kersting, and H. H. Yang, Phys. Rev. D **77**, 075011 (2008).
[28] F. Campanario, V. Hankele, C. Oleari, S. Prestel, and D. Zeppenfeld, Phys. Rev. D **78**, 094012 (2008).
[29] G. Aad *et al.* (ATLAS Collaboration), J. Instrum. **3**, P07007 (2008).
[30] G. L. Bayatian *et al.* (CMS Collaboration), J. Phys. G **34**, 995 (2007).
[31] G. Bagliesi *et al.*, Report No. CERN-CMS-NOTE-2006-028, 2006.
[32] A. F. Saavedra (ATLAS Collaboration), Report No. ATL-PHYS-PROC-2009-007, 2009.
[33] J. M. Campbell, R. K. Ellis, and D. L. Rainwater, Phys. Rev. D **68**, 094021 (2003).
[34] T. Gleisberg, S. Hoche, F. Krauss, M. Schonherr, S. Schumann, F. Siegert, and J. Winter, J. High Energy Phys. 02 (2009) 007.
[35] T. Gleisberg and S. Hoche, J. High Energy Phys. 12 (2008) 039.
[36] M. Cacciari, G. P. Salam, and G. Soyez, J. High Energy Phys. 04 (2008) 063.
[37] A. Buckley *et al.*, arXiv:1003.0694.
[38] M. Cacciari and G. P. Salam, Phys. Lett. B **641**, 57 (2006); M. Cacciari, G. P. Salam, and G. Soyez, http://fastjet.fr.
[39] H. Baer, V. Barger, G. Shaughnessy, H. Summy, and L. T. Wang, Phys. Rev. D **75**, 095010 (2007).

[40] H. Baer, H. Prosper, and H. Summy, Phys. Rev. D **77**, 055017 (2008).
[41] T. Nattermann, K. Desch, P. Wienemann, and C. Zendler, J. High Energy Phys. 04 (2009) 057.
[42] J. Brau *et al.*, Report No. ILC-REPORT-2007-001, Report No. CERN-2007-006, 2007; A. Djouadi, J. Lykken, K. Monig, Y. Okada, M. J. Oreglia, and S. Yamashita, arXiv:0709.1893.